

ARTICLE



FoxO1 suppresses IL-10 producing B cell differentiation via negatively regulating Blimp-1 expression and contributes to allergic asthma progression

Song-Rong Wang^{1,11}, Ren-Dong Hu^{1,11}, Min Ma^{1,11}, Xing You², Haiyan Cui³, Yi He⁴, Damo Xu⁵, Zhi-Bin Zhao⁶, Carlo Selmi^{7,8}, M. Eric Gershwin⁹, Liang Li⁶✉ and Zhe-Xiong Lian^{1,10}✉

© The Author(s), under exclusive licence to Society for Mucosal Immunology 2022

IL-10-producing B cells (B10) are involved in the prevention of autoimmune and allergic responses but its mechanisms remain poorly understood. We took advantage of the ovalbumin-induced asthma mouse model to demonstrate that the activity of FoxO1 is upregulated in lung B cells and correlates inversely with B10 cells, while showing decreased activity in ex vivo and in vitro induced B10 cells. We further observed that FoxO1 deficiency leads to increased frequency of B10 cells. These observations have in vivo clinical evidence, as B cell specific FoxO1 deficiency leads to reduced lung eosinophils and asthma remission in mice, and there are reduced regulatory B cells and increased FoxO1 activity in B cells of asthma patients. Single cell RNA-sequencing data demonstrated a negative correlation between the expression of *Foxo1* and *Ii10* in B cells from the mouse spleen and lung and the human lung. For a biological mechanism, FoxO1 inhibits the expression of *Prdm1*, which encodes Blimp-1, a transcription factor of B10 cells. Our experimental evidence in both murine and human asthma demonstrates that FoxO1 is a negative regulator of B10 cell differentiation via negatively regulating *Prdm1* and its expression in B cells contributes to allergic asthma disease.

Mucosal Immunology (2022) 15:459–470; <https://doi.org/10.1038/s41385-022-00504-z>

INTRODUCTION

Asthma is a chronic inflammatory disease largely mediated by T helper type 2 (Th2) cells¹ which accumulate in the airways and release cytokines such as IL-4, IL-5, IL-9, and IL-13, in turn promoting eosinophilic inflammation and immunoglobulin E (IgE) production. IgE triggers the release of inflammatory mediators such as histamine and cysteinyl leukotrienes, causing bronchospasm, edema, and increased mucous secretion^{2,3}. On the other hand, the immune tolerance breakdown is associated with Th2-driven, allergen-induced airway diseases. Regulatory B (Breg) cells are critical components of the suppressive immune cells, and can prevent the development of delayed-type hypersensitivity⁴ and allergic asthma⁵.

Due to the lack of uniform markers, several Breg subsets have been described with similar functions⁶, including the B10 subpopulation which produces IL-10 to suppress asthma⁷. The forkhead box O (FoxO) transcription factors are key to the evolutionarily conserved pathways involved in cell growth, proliferation, and differentiation⁸. In B cells, FoxO1 regulates the transcriptional program of early B cell development and peripheral B

cell function⁹ and instructs a gene program for the development of the germinal center dark zone¹⁰. FoxO1 is a downstream molecule of the PI3K-AKT signaling pathway leading to IL-10 production in B cells¹¹. Thus, FoxO1 may be a critical regulator of B10 cell differentiation.

Prdm1, which encodes Blimp-1, was also reported to regulate the generation, differentiation, and IL-10 production of B cells¹². In classical Hodgkin lymphoma (cHL), FoxO1 directly upregulates the full-length isoform PRDM1α in cHL cell lines. At the same time, a positive correlation between FOXO1 and PRDM1 expression levels in primary Hodgkin-Reed-Sternberg cells was observed¹³. FoxO1 deficiency also results in increased Blimp-1 expression in germinal center B cells and CD8⁺T cells^{10,14}. These studies suggest that FoxO1 may regulate IL-10 production of B cells through suppressing the expression of *Prdm1*.

In the present study, we investigated the involvement of FoxO1 in the B cell mediated tolerance in an asthma model and in patients, and we report that FoxO1 suppresses the B10 cell differentiation via negatively regulating Blimp-1 and promotes allergic asthma.

¹Chronic Disease Laboratory, School of Medicine, South China University of Technology, Guangzhou, China. ²School of Biomedical Sciences and Engineering, South China University of Technology, Guangzhou International Campus, Guangzhou 511442, P. R. China. ³Department of Respiratory and Critical Care Medicine, The Third Affiliated Hospital of Southern Medical University, Guangzhou, Guangdong 510630, China. ⁴Department of Rheumatology and Immunology, The Third Affiliated Hospital, Southern Medical University, Guangzhou, Guangdong 510630, China. ⁵State Key Laboratory of Respiratory Disease for Allergy at Shenzhen University, Shenzhen Key Laboratory of Allergy & Immunology, Shenzhen University School of Medicine, Shenzhen, China. ⁶Medical Research Center, Guangdong Provincial People's Hospital, Guangdong Academy of Medical Sciences, Guangzhou, China. ⁷Rheumatology and Clinical Immunology, Humanitas Clinical and Research Center—IRCCS, Rozzano, Milan, Italy. ⁸Department of Biomedical Sciences, Humanitas University, Milan, Italy. ⁹Division of Rheumatology, Allergy and Clinical Immunology, University of California at Davis School of Medicine, Davis, CA, USA. ¹⁰Guangdong Provincial People's Hospital, Guangdong Academy of Medical Sciences, Guangzhou, China. ¹¹These authors contributed equally: Song-Rong Wang, Ren-Dong Hu, Min Ma. ✉email: lil2009@mail.ustc.edu.cn; zxl1@ustc.edu.cn

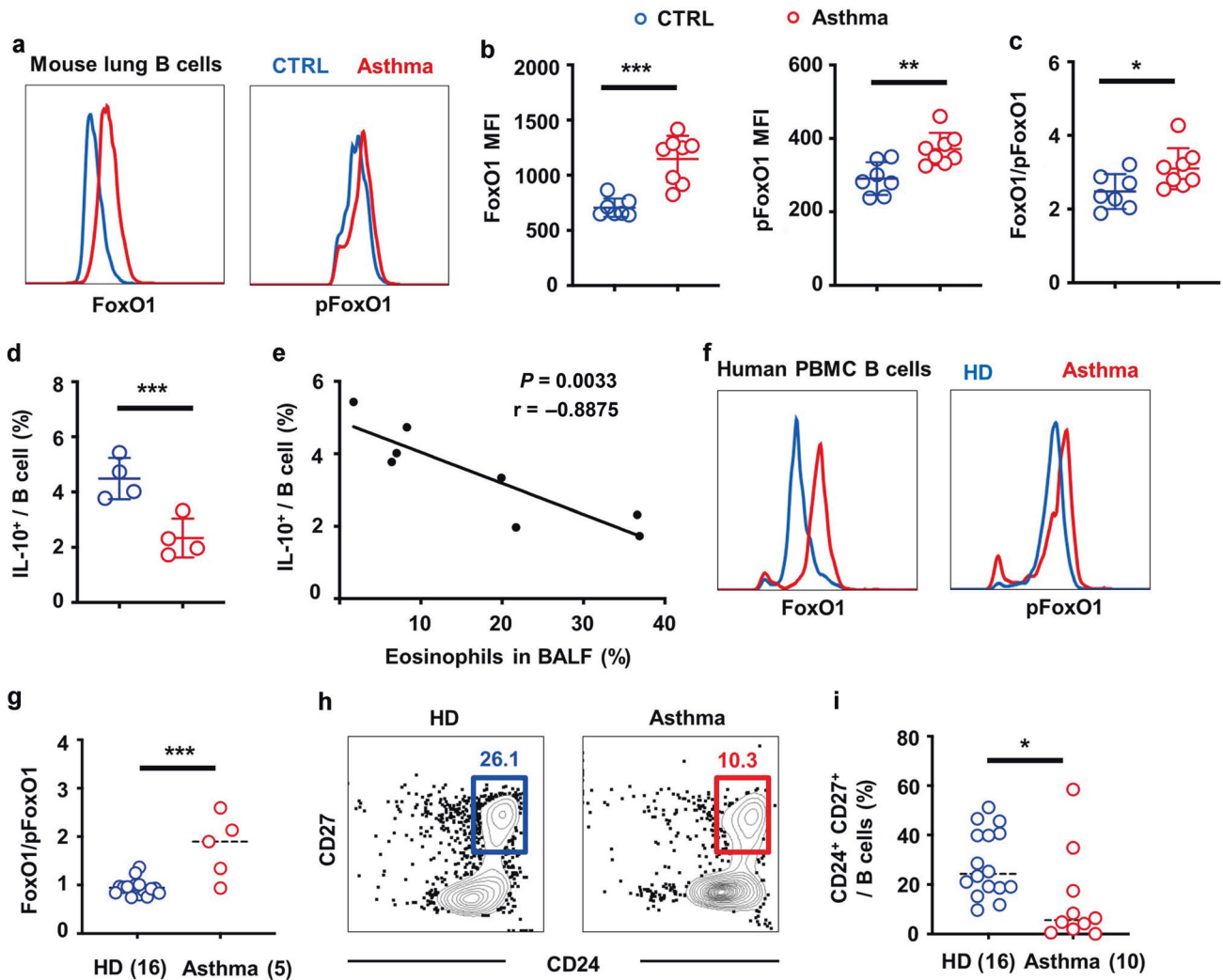


Fig. 1 Increased FoxO1 activity in B cells and decreased B10 cells in OVA-induced asthma model and asthma patients. **a** FoxO1 and pFoxO1 expression in lung B cells from control and asthma mice detected by flow cytometry; **b** FoxO1 and pFoxO1 expression level (MFI) in lung B cells from control ($n = 7$) and asthma ($n = 8$) mice; **c** FoxO1/pFoxO1 levels in lung B cells from control ($n = 7$) and asthma ($n = 8$) mice; **d** B10 cell frequency among lung B cells from control ($n = 4$) and asthma ($n = 4$) mice; **e** Correlation between the percentage of BALF eosinophils and lung B10 cells ($n = 8$); **f** The FoxO1 and pFoxO1 level of B cell of patients with asthma and healthy donors; **g** The activity of FoxO1 on B cells of asthma patients ($n = 5$) and healthy donors ($n = 16$); **h** Representative flow cytometry result of the frequency of CD24⁺CD27⁺ cells in B cells from a patient with asthma and a healthy donor; **i** The percentage of CD24⁺CD27⁺ cell in B cells from patients with asthma ($n = 10$) and healthy donors ($n = 16$). Data from mice were collected at day 28 after asthma induction. Data in this figure are representative of three independent experiments. * $p < 0.05$, ** $p < 0.01$, *** $p < 0.001$.

RESULTS

Increased FoxO1 activity in B cells and decreased B10 cells in OVA-induced asthma model and asthma patients

FoxO1 participates in multiple parts of B cell differentiation, but little is known about its role in regulating their suppressive function, especially in allergic asthma disease. We induced asthma in mice with ovalbumin (OVA) (Supplementary Fig. 1a)¹⁵ and detected the expression of FoxO1 and phosphorylated FoxO1 (pFoxO1) in lung B cells. FoxO1 can be phosphorylated and exported from nuclei to the cytoplasm for degradation^{16,17}. We found that compared with control mice, both FoxO1 and pFoxO1 levels were increased in lung B cells (Fig. 1a, b). However, FoxO1/pFoxO1 level was increased (Fig. 1c), indicating elevated FoxO1 activity of lung B cells during asthma development. Meanwhile, we also observed increased FoxO1 activity in spleen B cells after asthma induction (Supplementary Fig. 1b).

In the mouse asthma model, B10 cells take part in limiting Th2 type immune response¹⁸. We also found decreased B10 cells in

lungs (Fig. 1d) and spleens (Supplementary Fig. 1c) of mice with asthma. Furthermore, there was a negative correlation between the percentage of B10 cells in the lung and the percentage of eosinophils in BALF, which reflects the severity of asthma disease (Fig. 1e).

We then detected FoxO1 activity of peripheral blood mononuclear cells (PBMCs) and Breg cell percentage from asthma disease ($n = 10$) and healthy donors ($n = 16$). We found that FoxO1 activity in B cells was upregulated in asthma patients, which is consistent with the observation in our murine asthma model (Fig. 1f, g). B10 cells in human are identified by surface markers (CD19⁺CD24⁺CD27⁺)⁶. We also found the frequency of Breg cells in asthma patients was much lower than that of healthy donors (Fig. 1h, i), which is consistent with previous studies¹⁹ and the observation in our murine asthma model.

Taken together, our results demonstrate that increased FoxO1 activity in B cells is associated with decreased B10 cells in OVA-induced asthma model and asthma patients.

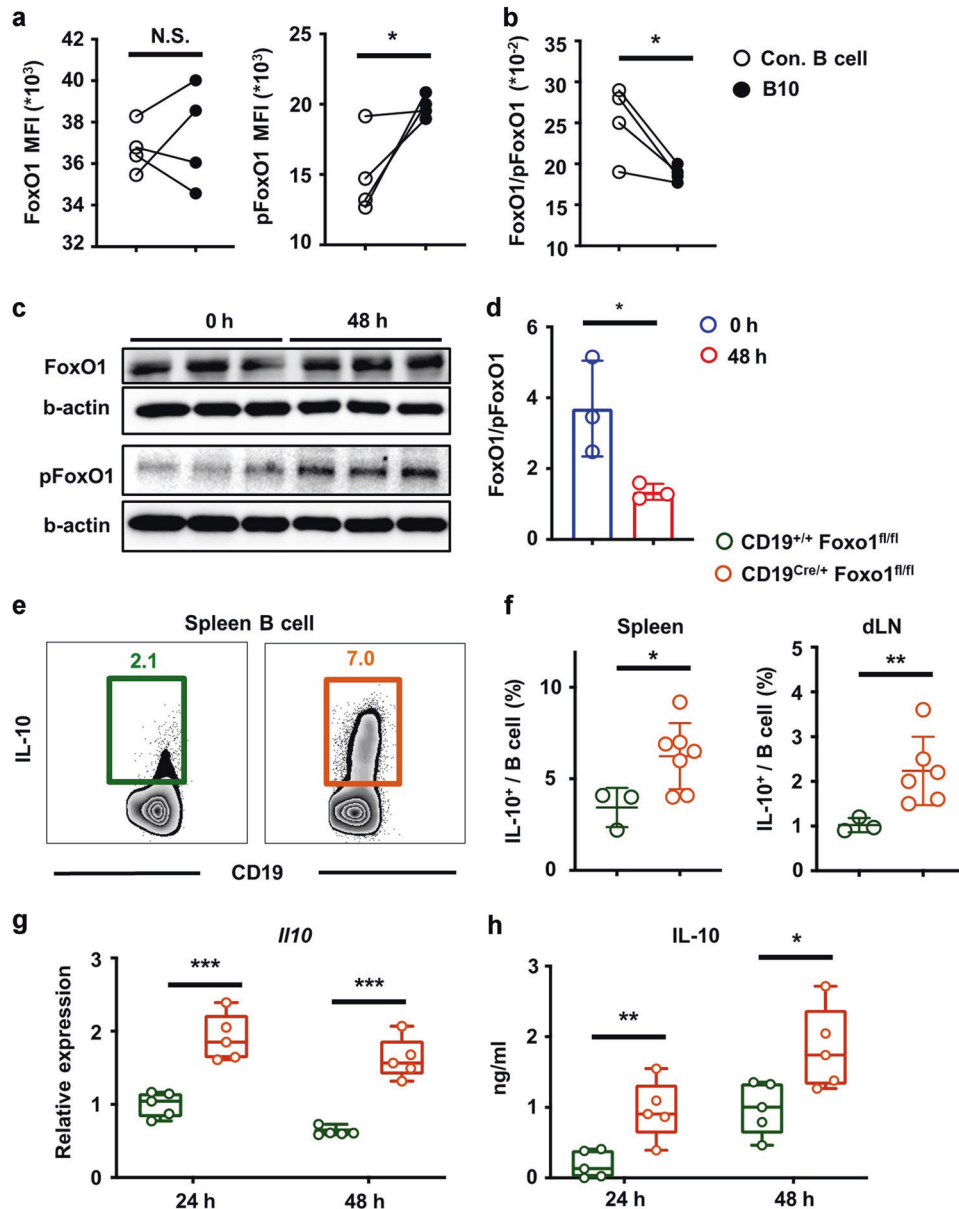


Fig. 2 B10 cells manifest decreased FoxO1 activity. **a, b** FoxO1 and FoxO1 expression in IL-10-producing and conventional B cells from the spleen of wild type mice ($n = 4$); **(c)** Western blot result of FoxO1 and pFoxO1 protein level of B cells stimulated with LPS for 0 h and 48 h; **(d)** FoxO1/pFoxO1 expression level of B cells stimulated with LPS for 0 h and 48 h; **(e)** IL-10⁺ B cells in the spleen of CD19^{Cre/+} Foxo1^{fl/fl} mice and CD19^{+/+} Foxo1^{fl/fl} mice; **(f)** The percentage of B10 cells in spleen and lymph nodes of CD19^{Cre/+} Foxo1^{fl/fl} mice ($n = 7$) and CD19^{+/+} Foxo1^{fl/fl} mice ($n = 3$); **(g)** *Il10* mRNA level of B cells from CD19^{Cre/+} Foxo1^{fl/fl} mice ($n = 5$) and CD19^{+/+} Foxo1^{fl/fl} mice ($n = 5$) stimulated with LPS for 24 h and 48 h; **(h)** IL-10 concentration in the supernatant of B cells from CD19^{+/+} Foxo1^{fl/fl} mice ($n = 5$) and CD19^{+/+} Foxo1^{fl/fl} mice ($n = 5$) stimulated with LPS for 24 h and 48 h. Data in this figure are representative of two independent experiments. * $p < 0.05$, ** $p < 0.01$, *** $p < 0.001$.

B10 cells have decreased FoxO1 activity

To further investigate the relationship between FoxO1 and B10 cell differentiation, we detected the FoxO1 and pFoxO1 level in B10 cells and conventional B cells in the spleens of WT mice. The FoxO1 level was similar between B10 cells and conventional B cells. However, the pFoxO1 level was higher in B10 cells (Fig. 2a). The FoxO1/pFoxO1 level which indicates the activity of FoxO1 was lower in B10 cells than conventional B cells (Fig. 2b).

Further, we induced B10 cell differentiation from spleen B cells with LPS in vitro²⁰. The percentage of IL-10 producing B cells increased after 48 h stimulation (Supplementary Fig. 1d). We found the activity of FoxO1 was down-regulated in the process of B10 differentiation (Fig. 2c, d). To test whether IL-10 can be

induced antigen-specifically, we isolated spleen B cells from mice immunized with OVA and stimulated them with OVA in vitro. We found that OVA stimulation induced higher concentrations of IL-10 in the supernatant of B cells from OVA-immunized mice (Supplementary Fig. 1e). B cells from mice sacrificed at day 21 have a higher ability to secrete IL-10 than those from day 42 after immunization, possibly due to decreased antigen-specific memory B cells in the spleen (Supplementary Fig. 1e).

FoxO1 has previously been reported to play crucial roles in lymphocyte differentiation, especially the differentiation of immunosuppressive lymphocytes^{10,21–23}. To investigate the role of FoxO1 in B10 cell development, we generated CD19^{Cre/+}Foxo1^{fl/fl} mice, in which FoxO1 is specifically knocked out in B cells.

We found that the percentages of B10 cells in the spleen and dLN increased in CD19^{Cre/+}Foxo1^{fl/fl} mice compared with littermate CD19^{+/+}Foxo1^{fl/fl} mice (Fig. 2e, f). We also found the expression of CD1d, one of the B10 cell markers, increased in B cells from the spleen of CD19^{Cre/+}Foxo1^{fl/fl} mice compared with littermate CD19^{+/+}Foxo1^{fl/fl} mice (Supplementary Fig. 1f). Meanwhile, the expression of CD23, which is reported to negatively regulate B cell activation, was decreased in B cells from the spleen of CD19^{Cre/+}Foxo1^{fl/fl} mice compared with littermate CD19^{+/+}Foxo1^{fl/fl} mice (Supplementary Fig. 1g). We also sorted B cells from the spleen of CD19^{Cre/+}Foxo1^{fl/fl} mice and CD19^{+/+}Foxo1^{fl/fl} mice, and cultured for 24 h or 48 h with LPS. The *Il10* mRNA was upregulated after 24 h and 48 h culture (Fig. 2g). The IL-10 protein level in the supernatant, which reflects the IL-10 secreting capability, was also increased along with the culture process (Fig. 2h). Thus, the B cells from CD19^{Cre/+}Foxo1^{fl/fl} mice have increased IL-10 secreting capability compared with B cells from CD19^{+/+}Foxo1^{fl/fl} mice.

FoxO1 deletion in B cells results in ameliorated asthma

Then, we induced asthma in CD19^{Cre/+}Foxo1^{fl/fl} and control CD19^{+/+}Foxo1^{fl/fl} mice. BHR is regarded as a hallmark of asthma^{24,25}. We found that the CD19^{Cre/+}Foxo1^{fl/fl} mice showed alleviated airway responsiveness compared with control mice (Fig. 3a). The IgE level was also decreased in the serum and BALF of CD19^{Cre/+}Foxo1^{fl/fl} mice (Fig. 3b). However, the OVA-specific IgE level showed no significant change (Supplementary Fig. 1h). The pathology of the lungs showed decreased inflammatory cell infiltration around the bronchi and vessels, as well as mucus hypersecretion within the bronchi (Fig. 3c). The PAS staining also demonstrated less Goblet cells in the lung of CD19^{Cre/+}Foxo1^{fl/fl} mice (Fig. 3d). The lung pathology is characterized by decreased inflammatory cell infiltration around the bronchi and vessels in CD19^{Cre/+}Foxo1^{fl/fl} mice (Fig. 3e, f). We also found a decreased Th2 immune response in the lung of CD19^{Cre/+}Foxo1^{fl/fl} mice, as indicated by decreased IL-4 level (Fig. 3g).

FoxO1 deletion in B cells results in altered immune landscape of BALF and lung after asthma induction

Then, we detected the changes of immune cells in BALF and lung of mice with asthma. We used tSNE map to display CD45⁺ cells in BALF and different immune cell subsets were indicated as different colors (Fig. 4a). We observed a decrease of eosinophils (Eos) and an increase of alveolar macrophages (AM) in BALF from CD19^{Cre/+}Foxo1^{fl/fl} mice compared with control mice in tSNE plots (Fig. 4a). Statistically, Eos percentage was significantly decreased and AM percentage was significantly increased, while the neutrophil percentage did not change in BALF (Fig. 4b). The percentages of B cells, CD4⁺ T cells and CD8⁺ T cells were similar between CD19^{Cre/+}Foxo1^{fl/fl} mice and control littermates (Supplementary Fig. 2a). The numbers of eosinophils, AM, Neu, CD4⁺ T cells and CD8⁺ T cells decreased in BALF from CD19^{Cre/+}Foxo1^{fl/fl} mice compared with control mice (Fig. 4b, Supplementary Fig. 2a).

We also used a tSNE map to display CD45⁺ cells in the lung (Fig. 4c). We observed a decrease of Eos and an increase of B cells in BALF from CD19^{Cre/+}Foxo1^{fl/fl} mice compared with control mice in tSNE plots (Fig. 4c). Statistically, the percentage of eosinophils in the lung was also decreased in CD19^{Cre/+}Foxo1^{fl/fl} mice (Fig. 4d). Unlike in the BALF, the percentage of AM cells decreased in the lungs of CD19^{Cre/+}Foxo1^{fl/fl} mice (Supplementary Fig. 2b). The percentages of DCs and T cells showed no significant difference in CD19^{Cre/+}Foxo1^{fl/fl} mice compared with control mice (Supplementary Fig. 2b). We found that B cells composed a large proportion of lung immune cells after asthma induction, and their percentage is higher in CD19^{Cre/+}Foxo1^{fl/fl} mice (Fig. 4c). There seemed to be two B cell clusters, mainly because B cells from CD19^{Cre/+}Foxo1^{fl/fl} mice have different CD19 expression from

CD19^{+/+}Foxo1^{fl/fl} mice. Intriguingly, we found that the percentage and number of B10 cells were increased in the lungs of CD19^{Cre/+}Foxo1^{fl/fl} mice (Fig. 4e, Supplementary Fig. 2c). Meanwhile, the IL-10 levels in the lung tissue and serum of CD19^{Cre/+}Foxo1^{fl/fl} mice were higher than in CD19^{+/+}Foxo1^{fl/fl} mice (Fig. 4f, g). We also found increased B10 cells in lung draining lymph nodes (Supplementary Fig. 2d), indicating an enhanced B10 cell response in the lung. Moreover, we found no difference in Treg cell percentage in the spleen, pLN (Supplementary Fig. 2e, f) and ILC2 percentage in lung (Supplementary Fig. 2g). Besides, there is no difference in Treg cell percentage in lungs between CD19^{Cre/+}Foxo1^{fl/fl} mice and control mice (Supplementary Fig. 2h). We also found that there was no difference in the expressions of IL-35 subunits *Il12a* and *Ebi3* in lungs from CD19^{Cre/+}Foxo1^{fl/fl} mice compared to control mice (Supplementary Fig. 2i). These results demonstrate that FoxO1 deficiency in B cells leads to alleviated asthma disease in mice, which is attributed to increased B10 cells.

FoxO1 negatively regulates B10 cell differentiation through suppressing *Prdm1* expression

To understand the heterogeneity of FoxO1 and IL-10 expression in B cells, and find the possible mechanism underlying B10 cell differentiation, we analyzed single cell RNA-sequencing (scRNA-seq) data of mouse (GSE132042) (Fig. 5a) and human (PRJEB31843) lung B cells (Fig. 5b). We identified four B cell clusters in WT mouse lung B cells (Fig. 5a). We found that *Foxo1* is highly expressed in clusters 0 and 3, while *Il10* is highly expressed in clusters 1 and 2. Interestingly, we found a positive correlation of *Il10* expression with *Prdm1* (Fig. 5c), which encodes the transcription factor Blimp-1. Blimp-1 has been reported to promote the development of Breg cells.²⁶ We identified four B cell clusters in human lung B cells (Fig. 5b). We found that *FOXO1* is highly expressed in clusters 1 and 2, while *IL10* is highly expressed in clusters 0 and 3. Interestingly, we also found a positive correlation of *IL10* expression with *PRDM1* (Fig. 5d). We also analyzed our scRNA-seq data of spleen B cells from WT mice (GSE174739), and identified five B cell clusters (Supplementary Fig. 3a). We found that the expression pattern was similar between mouse and human lung B cells. Clusters 1, 0 and 4 have high *Foxo1* expression and low *Prdm1* and *Il10* expression, while clusters 2 and 3 have high *Prdm1* and *Il10* expression and low *Foxo1* expression (Supplementary Fig. 3b).

To rule out the developmental deficiency of B cell subsets in CD19^{Cre/+}Foxo1^{fl/fl} mice, we treated B cells from spleens of WT mice with FoxO1 inhibitor AS1842856. The inhibiting efficacy of FoxO1 was measured by RT-PCR (Supplementary Fig. 3c). We found that both LPS and AS1842856 can induce *Il10* expression in B cells, and they act in a synergetic manner (Fig. 5e). Interestingly, we found that LPS and AS1842856 treatment could also induce *Prdm1* expression in B cells (Fig. 5e), suggesting that FoxO1 suppresses *Il10* expression through negatively regulating *Prdm1* expression.

We then used *Prdm1* shRNA to knockdown *Prdm1* in sorted spleen B cells from WT mice. We found that FoxO1 inhibitor could increase *Il10* mRNA expression. Interestingly, the effect was abrogated by *Prdm1* knockdown (Fig. 5f). The in vitro experiments demonstrate that FoxO1 suppresses B10 cell differentiation through negatively regulating the expression of *Prdm1*.

Transfer of FoxO1 deficient B cells to WT mouse alleviates allergic asthma disease

FoxO1 is critical for B cell antibody production²⁷. To investigate whether FoxO1 deficiency can affect IgE antibody production by B cells, we stimulated B cells in vitro with anti-CD40 and IL-4 to induce IgE class switching. We found that FoxO1 deficient B cells have decreased IgE production compared with WT B cells (Supplementary Fig. 4a). Treatment with FoxO1 inhibitor AS1842856 also led to

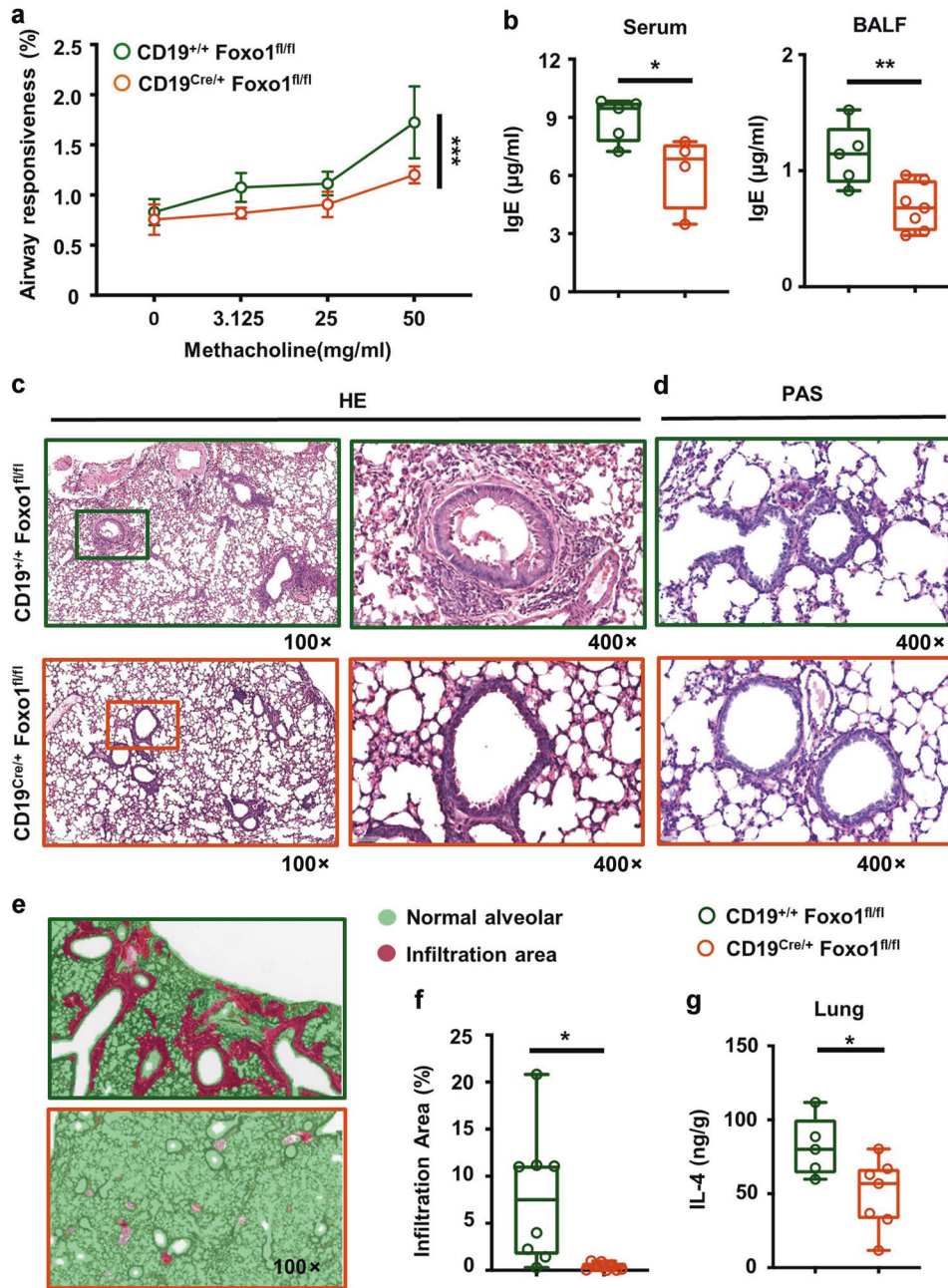


Fig. 3 Deletion of FoxO1 in B cells ameliorates asthma. **a** BHR results of CD19^{Cre/+} Foxo1^{fl/fl} mice ($n = 4$) and CD19^{+/+} Foxo1^{fl/fl} mice ($n = 4$); **(b)** Serum IgE levels of CD19^{Cre/+} Foxo1^{fl/fl} mice ($n = 4$) and CD19^{+/+} Foxo1^{fl/fl} mice ($n = 5$); BALF IgE levels of CD19^{Cre/+} Foxo1^{fl/fl} mice ($n = 7$) and CD19^{+/+} Foxo1^{fl/fl} mice ($n = 5$); **(c)** HE staining results of lung tissues of CD19^{Cre/+} Foxo1^{fl/fl} mice and CD19^{+/+} Foxo1^{fl/fl} mice; **(d)** PAS staining results of lung tissues of CD19^{Cre/+} Foxo1^{fl/fl} mice and CD19^{+/+} Foxo1^{fl/fl} mice; **(e)** Definition and quantification of infiltration area and normal alveolar of lung tissues from CD19^{Cre/+} Foxo1^{fl/fl} mice and CD19^{+/+} Foxo1^{fl/fl} mice using inForm software; **(f)** The percentages of infiltration area of lung tissues from CD19^{Cre/+} Foxo1^{fl/fl} mice and CD19^{+/+} Foxo1^{fl/fl} mice using inForm software. **(g)** Concentrations of IL-4 in lung tissues of CD19^{Cre/+} Foxo1^{fl/fl} mice ($n = 7$) and CD19^{+/+} Foxo1^{fl/fl} mice ($n = 5$). All data were collected at day 28 after asthma induction. Data in this figure are representative of two independent experiments. * $p < 0.05$, ** $p < 0.01$, *** $p < 0.001$.

decreased IgE production by B cells (Supplementary Fig. 4b). IL-10 is reported to inhibit IL-4 induced IgE production by human B cells²⁸. We found that IL-10 can also suppress IgE production in our system (Supplementary Fig. 4c, d), suggesting that FoxO1 deficiency mediated IL-10 over-expression, which may in turn suppress IgE production by B cells.

To investigate whether FoxO1 deficient B cells can suppress allergic asthma progression independent of IgE production, we induced asthma in WT mice and transferred with B cell from CD19^{Cre/+}

+ Foxo1^{fl/fl} and Foxo1^{fl/fl} mice 1 day before intranasal OVA challenge (Supplementary Fig. 5a). Neither of these two kinds of B cells had encountered OVA before adoptive transfer. We found that the frequency of B10 cells in the lung was higher in mice that received FoxO1 deficient B cells (Fig. 6a, b). Serum IgE level was lower in mice that received FoxO1 deficient B cells (Fig. 5c). PAS staining results showed fewer Goblet cells in the lungs of mice that received FoxO1 deficient B cells (Fig. 5d). Moreover, the level of Th2 cytokine IL-4 was lower in lungs from mice that received FoxO1 deficient B cells,

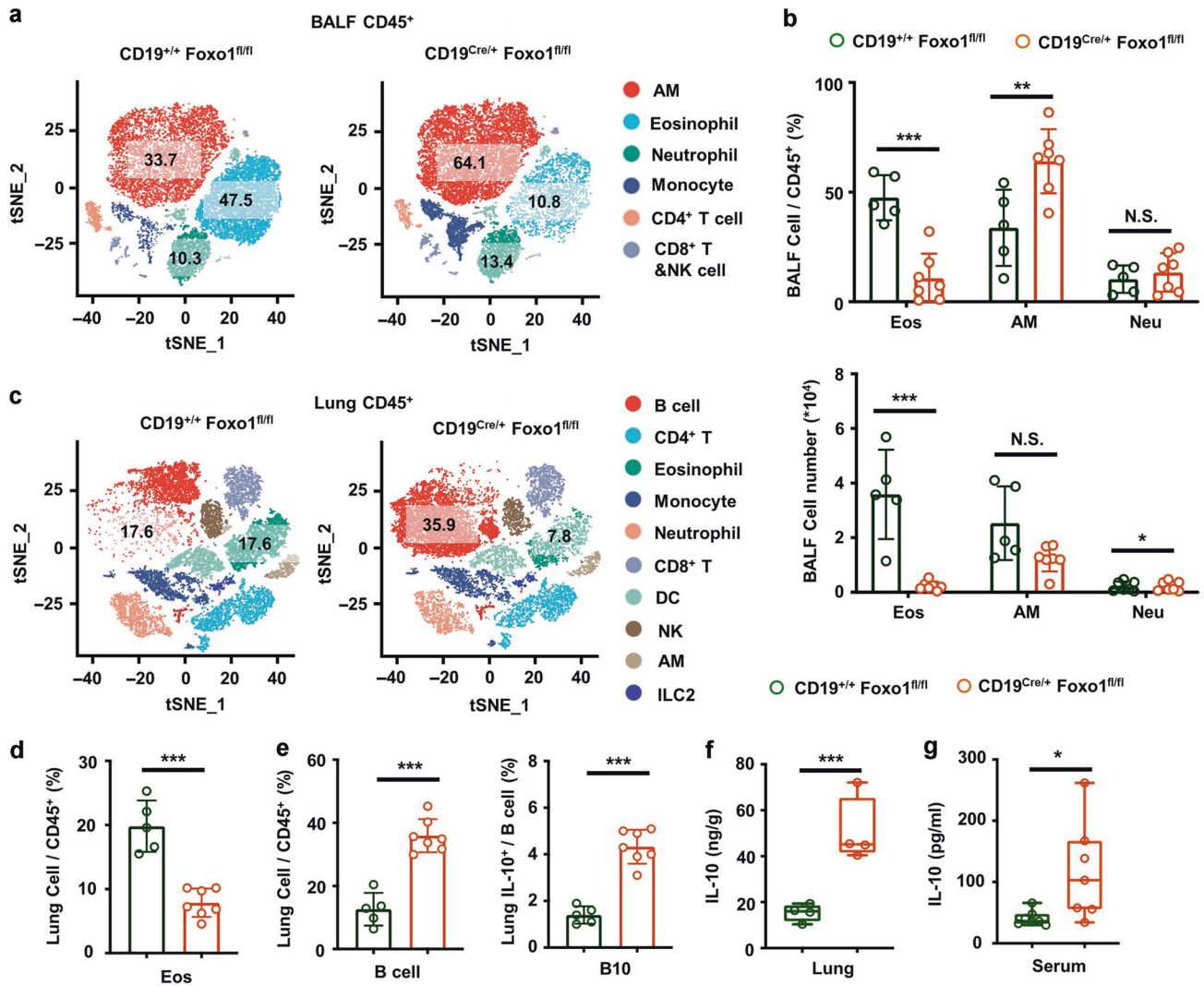


Fig. 4 BALF and lung cytology of CD19^{Cre/+} Foxo1^{fl/fl} mice and control littermates after asthma induction. **a** tSNE plot showing the composition of CD45⁺ immune cells of BALF from CD19^{Cre/+} Foxo1^{fl/fl} mice ($n = 3$) and CD19^{+/+} Foxo1^{fl/fl} mice ($n = 3$) after asthma induction; **(b)** The percentage and cell number of eosinophils (Eos), alveolar macrophages (AM) and neutrophils (Neu) of BALF from CD19^{Cre/+} Foxo1^{fl/fl} mice ($n = 7$) and CD19^{+/+} Foxo1^{fl/fl} mice ($n = 5$) after asthma induction; **(c)** tSNE plot showing the composition of CD45⁺ immune cells of lung from CD19^{Cre/+} Foxo1^{fl/fl} mice ($n = 3$) and CD19^{+/+} Foxo1^{fl/fl} mice ($n = 3$) after asthma induction. **(d)** Percentage of eosinophils (Eos) in the lung of CD19^{Cre/+} Foxo1^{fl/fl} mice ($n = 7$) and CD19^{+/+} Foxo1^{fl/fl} mice ($n = 5$) after asthma induction; **(e)** Percentages of B cells and B10 cells in the lung of CD19^{Cre/+} Foxo1^{fl/fl} mice ($n = 7$) and CD19^{+/+} Foxo1^{fl/fl} mice ($n = 5$) after asthma induction; **(f)** IL-10 concentrations in lung tissues of CD19^{Cre/+} Foxo1^{fl/fl} mice ($n = 4$) and CD19^{+/+} Foxo1^{fl/fl} mice ($n = 4$) after asthma induction; **(g)** IL-10 concentrations in serum of CD19^{Cre/+} Foxo1^{fl/fl} mice ($n = 7$) and CD19^{+/+} Foxo1^{fl/fl} mice ($n = 7$) after asthma induction. All data were collected at day 28 after asthma induction. Data in this figure are representative of two independent experiments. * $p < 0.05$, ** $p < 0.01$, *** $p < 0.001$.

indicating a decreased Th2 response (Fig. 5e). We found that the number, but not percentage, of Eos is lower in BALF of mice that received FoxO1 deficient B cells compared with mice that received WT B cells (Fig. 5f). The percentage of AM is higher, but the cell number is lower in BALF (Fig. 5f). Interestingly, we found a lower percentage and number of neutrophils in BALF, suggesting a remission of inflammation in the lung. In the lung tissue, the percentage and number of Eos were lower in mice that received FoxO1 deficient B cells, but there was no significant change in the percentage and number of AM and neutrophils (Fig. 5h). We found that the transfer of FoxO1 deficient B cells did not change systemic B cell IL-10 production, as the percentage of IL-10⁺ B cells in the spleen was comparable between mice that received two different B cells (Supplementary Fig. 5b). This indicates that FoxO1 may regulate B cell function locally in the inflamed lung tissue. We found that the percentages and numbers of ILC2, and IL-10⁺CD4⁺ T cells showed no significant change (Supplementary

Fig. 5c–e), while the number of Treg cells decreased in mice that received FoxO1 deficient B cells.

To characterize the intrinsic effect of FoxO1 in B cells, we also performed mixed bone marrow (BM) chimera experiment. We reconstituted B cell deficient (μ MT) mice with BM cells from CD19^{Cre/+} Foxo1^{fl/fl} (CD45.2) and WT mice (CD45.1) (Supplementary Fig. 6a). We found that the frequency of B cells from CD19^{Cre/+} Foxo1^{fl/fl} mice were higher than that from WT mice in both lung and spleen (Supplementary Fig. 6b, c). Interestingly, the ratio of KO: WT B cells is about 4:1 in the lung, suggesting that FoxO1 deficient B cells have higher capacity to develop in the host and migrate to lung tissue.

DISCUSSION

Breg cells are regarded as B cells with suppressive function, but there is no unified marker or defined transcription factor defining

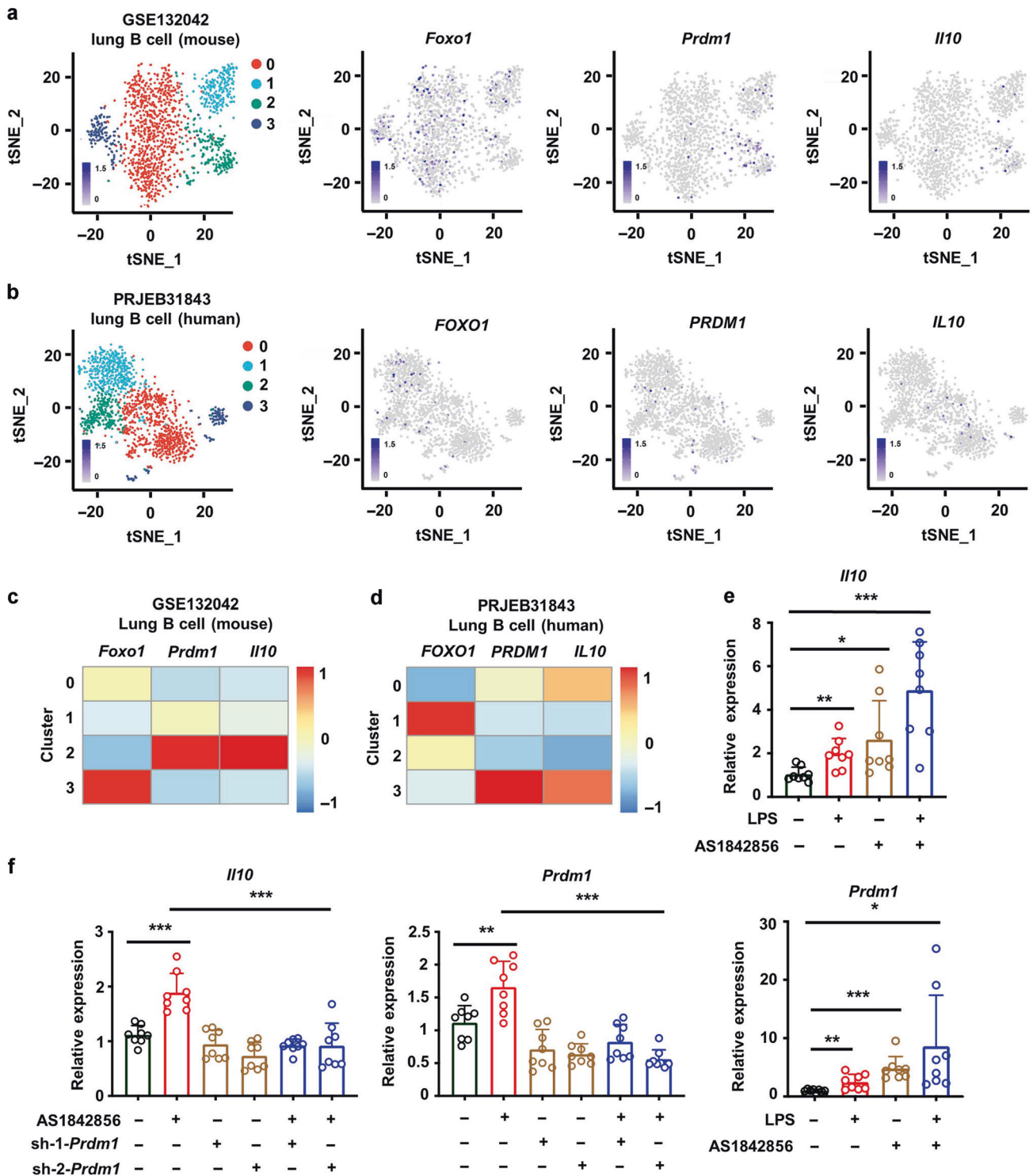


Fig. 5 FoxO1 negatively regulates B10 cell differentiation by suppressing *Prdm1* expression. **a** tSNE plot of B cells of mouse lung (GSE132042) and gene expression of *Foxo1*, *Prdm1*, and *Il10*; **(b)** tSNE plot of B cells of human lung (PRJEB31843) and gene expression of *FOXO1*, *PRDM1*, and *IL10*; **(c)** Heatmap of the expression of *Foxo1*, *Prdm1*, and *Il10* in different B cell clusters; **(d)** Heatmap of the expression of *FOXO1*, *PRDM1*, and *IL10* in different B cell clusters; **(e)** *Il10* and *Prdm1* expression of B cells stimulated with LPS, AS1842856 or in combination for 24 h; **(f)** *Il10* and *Prdm1* expression of B cells stimulated with LPS, in combine with AS1342656 or *Prdm1* shRNA for 48 h. Data in **(e)** and **(f)** are pooled from two independent experiments * $p < 0.05$, ** $p < 0.01$, *** $p < 0.001$.

this subset while several B cell subsets have been reported with similar phenotype and functions⁶, including one secreting IL-10. IL-10 is involved in the prevention of allergic diseases and autoimmune diseases^{29–31}, and the B10 subpopulation differentiates via unknown

pathways⁶ to participate in immune tolerance in the lung, thus inhibiting the development of allergic asthma^{5,32}.

We report herein that FoxO1 is a negative regulator of B10 cell differentiation and may represent a therapeutic target for allergic

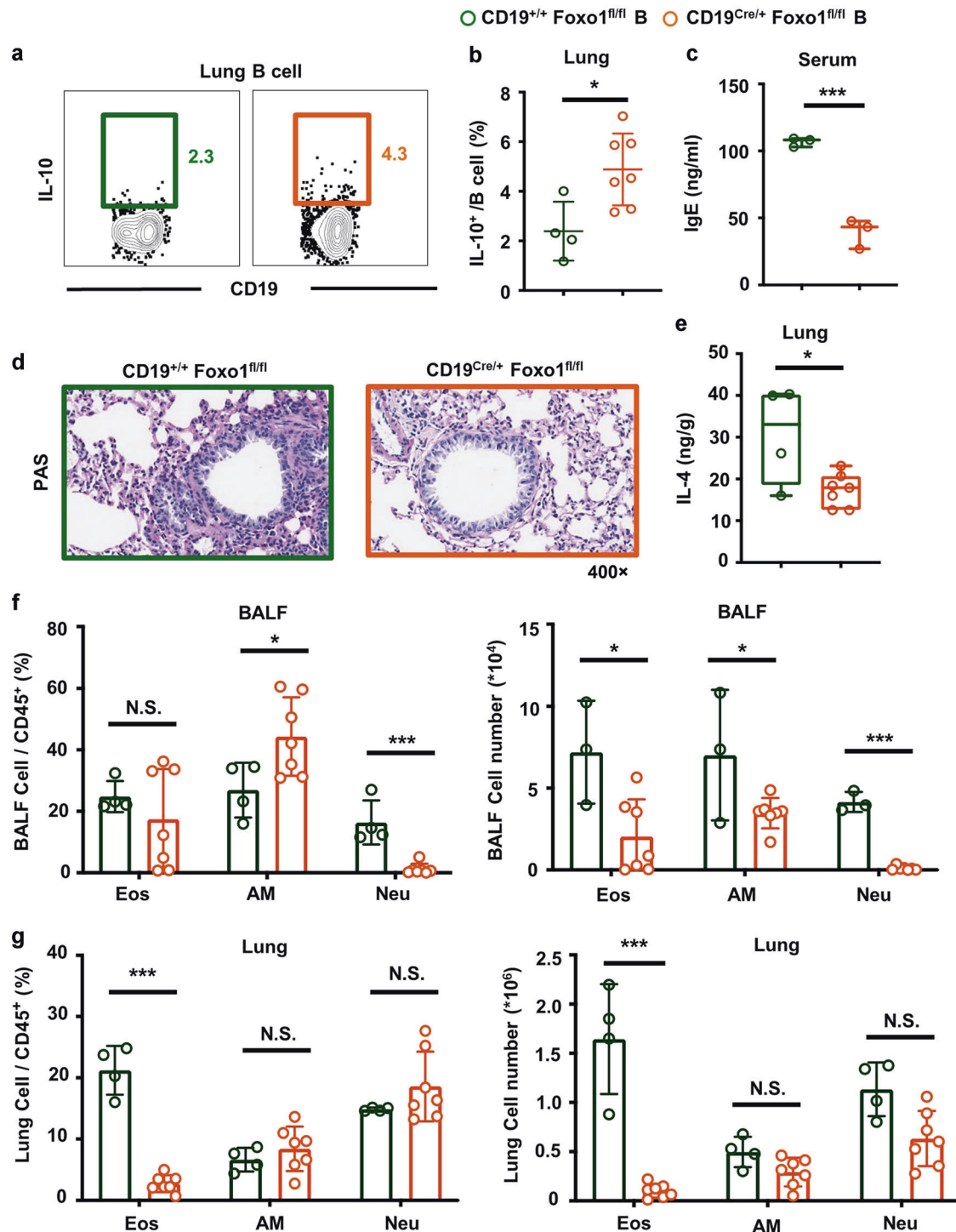


Fig. 6 Transfer of FoxO1 deficient B cells to WT mouse alleviates allergic asthma disease. Representative flow cytometry result (a) and statistic analysis (b) of IL-10 secreting B cells in the lung of mice receiving CD19^{Cre/+} Foxo1^{fl/fl} ($n = 7$) and CD19^{+/+} Foxo1^{fl/fl} ($n = 4$) B cells; (c) Serum IgE concentrations of mice receiving CD19^{Cre/+} Foxo1^{fl/fl} ($n = 3$) and CD19^{+/+} Foxo1^{fl/fl} ($n = 3$) B cells; (d) PAS staining results of lung tissues of mice receiving CD19^{Cre/+} Foxo1^{fl/fl} and CD19^{+/+} Foxo1^{fl/fl} B cells; (e) Concentrations of IL-4 in lung tissues of mice receiving CD19^{Cre/+} Foxo1^{fl/fl} ($n = 7$) and CD19^{+/+} Foxo1^{fl/fl} ($n = 4$) B cells; Percentage and numbers of eosinophils (Eos), alveolar macrophages (AM), and neutrophils (Neu) in BALF (f) and lung (g) of mice receiving CD19^{Cre/+} Foxo1^{fl/fl} ($n = 7$) and CD19^{+/+} Foxo1^{fl/fl} ($n = 4$) B cells. All data were collected at day 28 after asthma induction. Data in this figure are representative of two independent experiments. * $p < 0.05$. *** $p < 0.001$.

asthma. B10 cells appear to be activated rather than naive B cells derived from bone marrow⁶, while the PI3K-AKT pathway³³ is important for B cell activation and participates in Breg cell development, mediated by the effector role of FoxO1³⁴. Besides

acting on B cell lineage, FoxO1 contributes to gluconeogenesis and the commitment of preadipocytes to adipogenesis³⁵, controls regulatory T cell development and function²¹, and promotes Th9 cell differentiation²² while regulating the polarization of myeloid

cells to the macrophage inflammatory phenotype in allergic diseases³⁶. The role of FoxO1 in the normal development and differentiation of B cells has been investigated extensively during the past decade³³. It has been proven to influence B cell proliferation and class switching, while being down-regulated in B cells following B-cell antigen receptor signaling. It is also correlated with mature B cell proportion, as illustrated by cells lacking FoxO1³⁷. We demonstrate that FoxO1 is a critical mediator of the PI3K-AKT signaling pathway to mediate B10 cell development with potential implications in asthma.

IL-10 is reported to play a critical role in suppressing the development of allergic asthma. IL-10 produced by B cells can suppress CD4⁺Th2 cells³⁸, induce Treg cell differentiation^{39,40}, suppress IgE production by B cells⁴¹, and suppress pro-inflammatory cytokine production by DCs in the lymph nodes⁴². In our study, we found FoxO1 deficiency-induced IL-10 production of B cells can alleviate allergic asthma with no change in Treg cells and ILCs. However, we observed decreased IL-4 level in the lungs, indicating a suppressed Th2 cell response. This may be the critical contributing factor of IL-10 mediated allergic asthma remission. Besides, in our adoptive transfer experiment, we found that only B cells in the lung exhibited increased IL-10 production, suggesting that IL-10 induction in B cells depends on local inflammatory stimulation. Interestingly, we found that IL-10 can be induced by OVA-specific stimulation of B cells, suggesting that Breg cells can be induced locally in the lung.

Among the factors regulating murine B cells, we note the deficiency of *Irf4* and *Prdm1* genes, which are necessary for plasma cell differentiation, leads to exacerbated experimental autoimmune encephalomyelitis⁴², while Blimp-1 contributes to the development of regulatory B cells²⁶. It has been reported that FoxO1 directly upregulates the full-length isoform PRDM1a in cHL cell lines¹³. However, we found that in both mouse and human B cells, *Foxo1* expression negatively correlated with *Prdm1* and *Il10*, and knockdown of *Prdm1* expression abrogated the effect of *Foxo1* downregulation-induced *Il10* expression. Thus, FoxO1 suppresses B10 cell differentiation through negatively regulating *Prdm1* expression.

AS1842856A is a selective FoxO1 inhibitor proven to attenuate asthma, likely mediated by the inhibition of Th9 cell differentiation²² and increased M2 macrophages³⁶. However, the target cell of AS1842856 in this model remains unknown, while B cells compose the largest immune cell population in lung tissue after asthma induction. Thus, the result of FoxO1 inhibitor treatment may also be affected by increased B10 cells, which maintain immune tolerance. We are also intrigued by the consistency of the observed changes in both our murine asthma model and in patients with asthma.

There are also several limitations in this study. First, we can't rule out the possibility of FoxO1 deficiency induced down-regulation of IgE production in allergic asthma remission. Second, the detailed mechanism of how FoxO1 regulate B10 cell development remains unknown. We observed significantly decreased CD23 expression in FoxO1 deficient B cells. Loss of CD23 expression can result in B cell activation and the increased phosphorylation of Erk, Akt and Btk⁴³. Erk activation is reported to control IL-10 secretion by B cells⁴⁴. Btk signaling also drives regulatory B cell differentiation in tumor microenvironment⁴⁵. The activation of these pathways may result in increased B10 cell differentiation. Third, regulatory B cells can arise from immature B cells, mature B cells, and plasmablasts⁴⁶. At which stage of B cell development or activation does FoxO1 regulate the development of Regulatory B cells remains unknown.

In conclusion, FoxO1 suppresses B10 cell development through inhibiting Blimp-1 expression and participates in the immunopathology of asthma in both murine and human asthma. Deleting FoxO1 in B cells can induce B10 cell differentiation and attenuate asthma. Our data collectively enhances our understanding of the immune tolerance mechanisms of allergic asthma.

MATERIALS AND METHODS

Mice

Starting in all cases from a C57BL/6 background, we investigated (i) the wild type (WT) purchased from Hunan SJA Laboratory Animal Co., LTD, (ii) LoxP-flanked FoxO1 (Foxo1^{fl/fl}) mice homozygous for a loxp allele of Foxo1 were kindly provided by Dr. Qinghua Shi (University of Science and Technology of China), (iii) B6.129S2-*Ighm*^{tm1Cgn/J} (μMT) mice, (iv) B6.SJL-*Ptprc*^a *Pepc*^b/BoyJ (CD45.1) mice, and (v) CD19^{Cre/+}Foxo1^{fl/fl} and Foxo1^{fl/fl} littermates moving from CD19-cre mice were initially purchased from the Jackson Laboratory. All mice were housed and bred in Laboratory Animal Research Center, South China University of Technology (SCUT) under a specific pathogen-free condition. Animal experiments were approved by the Ethics Committee on Animal Use and performed according to guidelines for experimental animals in SCUT. 6- to 12-weeks old mice were used in this study.

We used 6-8 week-old male wild type, CD19^{Cre/+}Foxo1^{fl/fl} and control littermate mice to induce asthma using 50 μg OVA (Sigma-Aldrich, German) emulsified with 2 mg Imject™ Alum Adjuvant (Thermo Fisher Scientific, USA) in 100 μl 1× phosphate buffer saline (PBS) at day 0, 7, and 14. Mice were treated intranasally with 50 mg/ml OVA in 30 μl 1×PBS at day 14, 25, 26, 27 and sacrificed at day 28.

Subjects

Peripheral blood samples were obtained from patients with acute asthma prior to any medical treatment ($n = 15$) and healthy subjects ($n = 16$) enrolled at The Third Affiliated Hospital of Southern Medical University (Guangzhou, China). The study was approved by the ethics committee of The Third Affiliated Hospital of Southern Medical University, and informed consents were obtained from all patients and healthy donors.

Asthma patients were diagnosed by clinical doctors and defined as having a clear history of relevant clinical symptoms with either reversible airways obstruction ($\geq 15\%$ variability in the FEV1 either spontaneously or after inhaled albuterol, 200 μg), and/or a histamine PC20 provocation test result < 8 mg/mL documented in the previous 6 months. Healthy controls were defined as having a lifelong absence of asthma symptoms, FEV1 within the predicted range, and $< 5\%$ reversible with bronchodilator. Other information is listed in Table 1.

Cell isolation

Mice were sacrificed by CO₂ inhalation and after removing the muscle layer around the neck to expose the trachea, the lungs were filled and washed twice with 1 ml 1×PBS. After the BALF fluid was obtained, BALF cell numbers were counted using flow cytometry and the lung was perfused by quickly injecting 2.5 ml 1×PBS into the right atrium. Lungs were then cut and digested in RPMI 1640 medium (GE Healthcare Life Sciences, UK) containing 100 μg/ml LiberaseTL (Roche, Basel, Switzerland) and 100 μg/ml DNase I (Roche) with shaking for 30 min at 37 °C. Red blood cells were depleted using Red Blood Cell Lysis Buffer (Beyotime Biotechnology, Beijing, China). Lung draining lymph nodes, peripheral lymph nodes and spleens were grinded on ice with the rough surface of the glass slides in 1×PBS containing 0.2% bovine serum albumin. Bone marrow cells were flushed from femurs and tibias using a 2.5 ml syringe fitted with a 25-gauge needle. Red blood cells of the spleen were depleted using Red Blood Cell Lysis Buffer.

In the case of human samples, 2 ml of EDTA-anticoagulated peripheral blood was diluted to 4 ml with 1×PBS and the diluted peripheral blood was gently laid over an equal volume of Lymphprep™ (STEMCELL Technologies, Vancouver, Canada) solution in a 15 ml centrifuge tube and centrifuged at 800 g for 20 min. Mononuclear cell layer was collected and washed with 1×PBS.

Adoptive B cell transfer

Spleen B cells from CD19^{Cre/+}Foxo1^{fl/fl} and Foxo1^{fl/fl} mice were isolated by MACS using Mouse CD19 Microbeads (Miltenyi Biotec, Auburn, CA). 1×10^7 B cells were transferred to recipient mice intravenously at day 24 of asthma induction. Mice were sacrificed at day 28.

Bone marrow chimera

μMT mice were subjected to sublethal irradiation (5 Gy) before adoptive transfer (i.v.) of 5×10^5 bone marrow cells from CD19^{Cre/+}Foxo1^{fl/fl} (CD45.2) and 5×10^5 bone marrow cells from WT (CD45.1) mice. Mice were sacrificed at day 21 after reconstitution.

Table 1. Clinical information of asthma patients and healthy donors.

	Asthma(15)	HD(16)
Age(Mean/SD)	31.9	33.2
F/M	M(10) F(5)	M(8) F(8)
BMI	21.5	23.1
Age of asthma onset (y)	4.8	
Smoking status	Ever-smoker(4) Non-smoker(11)	Ever-smoker(3) Non-smoker(13)
Blood Eosinophil count (*10 ⁹ /L)	0.57	
Post-Bronchodilator FEV1 (% predicted)	76.3	

B cell culture in vitro

B cells from the spleen were isolated by MACS using Mouse CD19 Microbeads (Miltenyi Biotec) or sorted with FACS Aria III cell sorting system (BD Immunocytometry Systems, San Jose, CA, USA), obtaining cell purity > 90%. B cells were cultured in complete medium (RPMI 1640 medium containing 10% FBS, 1% HEPES, 1% L-glutamine, 1% Pen/Strep, and 0.1% 2-ME) and stimulated with sterile 10 µg/ml LPS (Sigma) and FoxO1 inhibitor AS1842856 1 µM (TargetMol, MA, USA) alone or with a combination of these compounds in Rsbiochem with 5% CO₂. Cells were collected at 24 or 48 h.

For induction of IgE production in vitro, 1 × 10⁶ B cells in 24-well plates were stimulated with 10 µg/ml anti-mouse CD40 antibody (BioLegend, San Diego, CA) and 25 ng/ml recombinant mouse IL-4 (BioLegend) for 4 days at 37 °C in 5% CO₂. In some experiments, 333 pg/ml Mouse IL-10 Recombinant Protein (Thermo Fisher Scientific) was added in the culture.

OVA antigen specificity

6–8-week-old male wild type mice were immunized with 50 µg OVA at days 0, 7, and 14. On day 21 and 42, spleen B cells were isolated and cultured with 1 µg/ml OVA in Rsbiochem with 5% CO₂ for 48 h. Supernatants were collected and IL-10 concentrations were detected by IL-10 ELISA kit (Thermo Fisher Scientific).

Lentivirus production, infection and shRNA knockdown

293T cells were transfected with the plasmids pLKO.1 (*Prdm1*-shRNA plasmid), pCMV-DR8.9, and pCMV-VSV-G in the presence of lipo8000 (C0533, Beyotime) following the manufacturer's instructions. Supernatants containing virus particles were collected 48 h post transfection, centrifuged at 800 × g for 10 min, filtered through a 0.45 µm filter, and stored at -80 °C. B cells from the spleen were infected with lentivirus in the presence of LPS (10 µg/ml). Gene levels were detected 48 h after infection.

Flow Cytometry

For surface marker staining, cell suspensions were incubated with purified anti-CD16/32 antibody (BioLegend) for 15 min at 4 °C, and then stained for 20 min at 4 °C with a cocktail of fluorochrome-conjugated antibodies against cell surface markers. Monoclonal antibodies (mAbs) including mouse BV421-CD3 (17A2), BV650-B220 (RA3-6B2), AF700-CD4 (RM4-5), APC-Ly6C (HK1.4), FITC-Ly6G (1A8), Percp-Cy5.5-CD11c (N418), PE-Dazzle594-NK1.1 (PK136), BV605-Gr-1 (RB6-8C5), BV711-CD19 (6D5), BV785-CD3 (17A2), Ax700-CD8a (53-6.7), APC-ST2 (DIH9), APC-Cy7-CD11c (N418), PE-Cy7-CD127 (A7R34), FITC-I-A/I-E (M5/114.15.2), Percp-Cy5.5-ICOS (C398.4 A), APC-Cy7-CD45.2 (104), PE-Cy7-CD11b (M1/70), BV605-B220 (RA3-6B2), BV650-NK1.1 (PK136), BV421-CD3 (17A2), Alexa Fluro 647-CD1d (1B1), PE-CD5 (53-7.3), PE-CF594-CD19 (1D3), FITC-B220 (RA3-6B2), PE-CD25 (PC61), and PE-IgE (RME-1) were obtained from BioLegend. mAbs against mouse V500-CD45.2 (104), PE-Siglec-F (E50-2440), V500-CD11b (M1/70), and BUV563-CD4 (GK1.5) were obtained from BD Biosciences.

mAbs including human BV421-CD45RO (UCHL1), BV605-CD123 (6H6), BV785-CD19 (SJ25C1), Alexa Fluro 700-CD8a (HIT8a), APC-CD11c (3.9), APC-Cy7-CD45 (HI30), PE-CD25 (M-A251), PE-CF594-CD11b (M1/70), PE-Cy5-CD56 (5.1H11), PE-Cy7-HLA-DR (LN3), APC-Cy7-CD45.2 (104), BB515-CCR7 (3D12), Percp-Cy5.5-CD16 (3G8), PE-CD27 (O323), PE-Dazzle594-CD24 (ML5), and FITC-CD38 (HIT2) were obtained from BioLegend. mAbs including human BUV395-CD14 (MqP9), BUV563-CD4 (SK3), BUV737-CD127 (UTHT2), and BUV737-CD4 (SK3) were obtained from BD Biosciences.

For cell surface staining, DAPI (BOSTER, Wuhan, China) was added 5 min before data acquisition. Cell suspensions were subjected to LSRFortessa flow cytometer (BD Immunocytometry Systems). For intracellular cytokine

staining, cells were stimulated with a Cell Stimulation Cocktail (plus protein transport inhibitors) (eBioscience, CA, USA) for 4 h, stained with antibodies against cell surface markers and fixed with a fixation/permeabilization buffer kit (BD Biosciences). APC-IL-10 (JES5-16E3) was obtained from BioLegend.

For intracellular staining, cells were stained with antibodies against cell surface markers and treated with Cytofix/Cytoperm™ Fixation/Permeabilization Kit (BD Biosciences) (for pFoxO1 and IgE) or Foxp3/Transcription Factor Staining Buffer Set (eBiosciences) (for FoxO1). Cells were then stained with antibodies against FoxO1 and pFoxO1, and then secondary antibody against rabbit IgG. Anti-FoxO1 antibody (2880s) and anti-pFoxO1 antibody (9461s) were purchased from Cell Signaling Technology (CST, Danvers, MA, USA). Alexa Fluro 647-conjugated secondary antibody was purchased from Life Technologies (Waltham, MA, USA).

Flow cytometry data analysis

Data were initially analyzed with FlowJo software (Tree Star, Inc, Ashland, USA). The T-distributed stochastic neighbor embedding (t-SNE) analysis was used to profile BALF and lung immune cell composition in R (version 4.0). The expression matrixes of CD45⁺ immune cells from three CD19^{Cre/+} Foxo1^{fl/fl} and three CD19^{+/+} Foxo1^{fl/fl} mice after asthma induction were exported from FlowJo for further analysis. 5000 cells were randomly selected from each sample, then merged into one single matrix. Normalized expression matrix run T-SNE algorithm by RunTSNE function in Seurat package (version 3.0.1).

Quantitative real time PCR and serum tests

Total RNA was extracted using Trizol Reagent (Invitrogen, Carlsbad, CA) and the PrimeScript RT Reagent Kit with gDNA Eraser (TaKaRa, Japan) used for reverse transcription. SYBR Premix Ex Taq II (Takara) was used to perform quantitative real-time PCR. Gene expression values were normalized to control gene encoding β-actin (ΔCt). All results were calculated by the 2^(-ΔΔCt) method. The following oligonucleotides were used:

Il10: 5'- GCTCTACTGACTGGCATGAG -3' (sense) and 5'- CGCAGCTCTA GGAGCATGTG -3' (antisense);
Actb: 5'-GGCTGTATCCCTCCATCG -3' (sense) and 5'- CCAGTTGGTA ACAATGCCATGT -3' (antisense);
Prdm1: 5'-TTCTCTGGAAAAACGTGTGGG-3' (sense) and 5'- GGAGCC GGAGCTAGACTTG -3' (antisense);
Il12a: 5'- CTGTGCCTTGGTAGCATCTATG -3' (sense) and 5'- GCAGAG TCTCGCCATTATGATTC -3' (antisense);
Ebi3: 5'- GCTACAGGCTCGGTGGG -3' (sense) and 5'- GTGACATTTAGC ATGTAGGGCA -3' (antisense);

IL-10, IL-4, IgE, and OVA-specific IgE levels in serum and BALF were measured using IL-10 ELISA Kit (Thermo Fisher Scientific), IL-4 ELISA kit (Elabscience, China), IgE ELISA kit (Elabscience, China), and LEGEND MAX™ Mouse OVA Specific IgE ELISA Kit (BioLegend) according to the producers' instructions.

Western blot

For Western blot analysis, B cells were lysed with RIPA buffer (Beyotime Biotechnology), then supplemented with PMSF (Beyotime Biotechnology) and PhosSTOP (Roche). Total proteins were quantified with a Pierce BCA Protein Assay Kit (Thermo Fisher Scientific) and adjusted to a final concentration of 10 µg/µl. Primary antibodies for western blot analysis were as follows: anti-FoxO1, anti-phospho-FoxO1 and anti-beta actin. Secondary antibodies were HRP-linked anti-rabbit IgG, or HRP-linked anti-mouse IgG. All antibodies were purchased from CST. Western blot data were analyzed with ImageJ software (NIH, Bethesda, MD, USA).

scRNA-seq and data analysis

We sorted spleen B cells from WT mice and performed scRNA-seq with Single Cell 5' Library & Gel Bead Kit (10×genomics, Pleasanton, CA, USA). A gene expression library was constructed according to instructions from 10×genomics and sequenced by NovaSeq 6000 sequencing system (Illumina, San Diego, CA, USA). Sequencing data were processed with Cell Ranger (version 6.0) to acquire an expression matrix. Data were deposited into the GEO database under the accession number GSE174739. We also obtained scRNA-seq data of human lung parenchyma cells (PRJEB31843) and mouse lung cells (GSE132042) from the NCBI website. All data were analyzed using R software. For each dataset, expression matrix data were transformed into Seurat objects and t-distributed stochastic neighbor embedding (tSNE) of all cells were performed using the Seurat R

package (version 4.0). B cell cluster was extracted by gene expression feature *CD19* or *Cd19*. The gene expression level of *Foxo1*, *Prdm1* and *Il10* of each cell cluster were calculated and presented as heatmaps.

Non-invasive measurement of airway function and lung histology

Mice were placed in a whole-body chamber and basal readings were obtained and averaged for a 3 min period. Subsequently, increasing doses of methacholine (0–50 mg/ml) were aerosolized for 3 min, and readings were taken and averaged for 3 min after each nebulization.

For histology, lung samples were fixed in 4% paraformaldehyde and embedded with paraffin. Samples were cut into 4 μ m sections. After deparaffinization, sections were stained with hematoxylin and eosin (HE) or periodic acid-Schiff (PAS) for microscopic examination. HE stained slices of lung were scanned using a digital pathology slide scanner (Leica Biosystems, Nussloch, Germany) and viewed with inForm software (version 2.4.8, Akoya Biosciences, DE, USA). We defined the blank area, normal alveolar area, and inflammatory infiltration area of slices and trained the software to identify these areas. The infiltration area of different slices were then calculated automatically.

Statistical analysis

All experiments were conducted at least two times and data were taken from one representative experiment or pooled together. Continuous variables obtained from at least two replicates are presented as mean \pm standard deviation. Two-tailed student's *t* tests were used to identify significant differences. Differences were considered significant if the *P* value was <0.05 (**P* < 0.05 , ***P* < 0.01 , ****P* < 0.001).

DATA AVAILABILITY

The data that support the findings of this study are available on request from the corresponding author.

REFERENCES

- Holgate, S. T. Innate and adaptive immune responses in asthma. *Nat. Med.* **18**, 673–83. (2012).
- Lambrecht, B. N. & Hammad, H. The immunology of asthma. *Nat. Immunol.* **16**, 45–56 (2015).
- Rose, C. E. et al. Murine lung eosinophil activation and chemokine production in allergic airway inflammation. *Cell. Mol. Immunol.* **7**, 361–374 (2010).
- Katz, S., Parker, D. & Turk, J. B-cell suppression of delayed hypersensitivity reactions. *Nature* **251**, 550–551 (1974).
- Braza, F. et al. Regulatory functions of B cells in allergic diseases. *Allergy* **69**, 1454–1463 (2014).
- Rosser, E. C. & Mauri, C. Regulatory B cells: origin, phenotype, and function. *Immunity* **42**, 607–612 (2015).
- Hawrylyowicz, C. M. Regulatory T cells and IL-10 in allergic inflammation. *J. Exp. Med.* **202**, 1459–1463 (2005).
- Tia, N. et al. Role of Forkhead Box O (FOXO) transcription factor in aging and diseases. *Gene* **648**, 97–105 (2018).
- Dengler, H. S. et al. Distinct functions for the transcription factor Foxo1 at various stages of B cell differentiation. *Nat. Immunol.* **9**, 1388–1398 (2008).
- Dominguez-Sola, D. et al. The FOXO1 transcription factor instructs the germinal center dark zone program. *Immunity* **43**, 1064–1074 (2015).
- Matsushita, T. et al. A novel splenic B1 regulatory cell subset suppresses allergic disease through phosphatidylinositol 3-kinase–Akt pathway activation. *J. Allergy Clin. Immunol.* **138**, 1170–1182. e9 (2016).
- Wang, Y.-H. et al., Blimp-1 contributes to the development and function of regulatory B cells. *Front. Immunol.* 2019. **10** (1909).
- Vogel, M. J. et al. FOXO1 repression contributes to block of plasma cell differentiation in classical Hodgkin lymphoma. *Blood* **124**, 3118–3129 (2014).
- Hess Michelini, R. et al. Differentiation of CD8 memory T cells depends on Foxo1. *J. Exp. Med.* **210**, 1189–1200 (2013).
- Henderson, W. R. Jr et al. A role for cysteinyl leukotrienes in airway remodeling in a mouse asthma model. *Am. J. Respiratory Crit. Care Med.* **165**, 108–116 (2002).
- Matsuzaki, H. et al. Insulin-induced phosphorylation of FKHR (Foxo1) targets to proteasomal degradation. *Proc. Natl. Acad. Sci.* **100**, 11285–11290 (2003).
- Obsil, T. & Obsilova, V. Structure/function relationships underlying regulation of FOXO transcription factors. *Oncogene* **27**, 2263–2275 (2008).
- Amu, S. et al. Regulatory B cells prevent and reverse allergic airway inflammation via FoxP3-positive T regulatory cells in a murine model. *J. Allergy Clin. Immunol.* **125**, 1114–1124. e8 (2010).

- Wirz, O. F. et al. Comparison of regulatory B cells in asthma and allergic rhinitis. *Allergy* **74**, 815–818 (2019).
- Yanaba, K. et al. The development and function of regulatory B cells expressing IL-10 (B10 cells) requires antigen receptor diversity and TLR signals. *J. Immunol.* **182**, 7459–7472 (2009).
- Kerdiles, Y. M. et al. Foxo transcription factors control regulatory T cell development and function. *Immunity* **33**, 890–904 (2010).
- Buttrick, T. S. et al. Foxo1 promotes Th9 cell differentiation and airway allergy. *Sci. Rep.* **8**, 818 (2018).
- Ottens, K. et al. Foxo3 promotes apoptosis of B cell receptor-stimulated immature B cells, thus limiting the window for receptor editing. *J. Immunol.* **201**, 940–949 (2018).
- Pattemore, P. K. et al. The interrelationship among bronchial hyperresponsiveness, the diagnosis of asthma, and asthma symptoms. *Am. Rev. Respir. Dis.* **142**, 549–554 (1990).
- Vos, A.P. et al. Dietary supplementation with specific oligosaccharide mixtures decreases parameters of allergic asthma in mice. *Int. Immunopharmacol.* **7**, 1582–1587 (2007).
- Wang, Y.-H. et al. Blimp-1 contributes to the development and function of regulatory B cells. *Front. Immunol.* **10**, 1909 (2019).
- Dominguez-Sola, D. et al. The FOXO1 transcription factor instructs the germinal center dark zone program. *Immunity* **43**, 1064–1074 (2015).
- Evans, H. M. et al. Restraint of fumarate accrual by HIF-1 α preserves miR-27a-mediated limitation of interleukin 10 during infection of macrophages by *Histoplasma capsulatum*. *mBio* **12**, e0271021 (2021).
- Hussaarts, L. et al. Regulatory B-cell induction by helminths: implications for allergic disease. *J. Allergy Clin. Immunol.* **128**, 733–739 (2011).
- Kalampokis, I., Yoshizaki, A. & Tedder, T. F. IL-10-producing regulatory B cells (B10 cells) in autoimmune disease. *Arthritis Res. Ther.* **15**, S1 (2013).
- Boldison, J. et al. Dendritic cells license regulatory B cells to produce IL-10 and mediate suppression of antigen-specific CD8 T cells. *Cell. Mol. Immunol.* **17**, 843–855 (2020).
- Yang, M. et al. Regulatory B cells in autoimmune diseases. *Cell. Mol. Immunol.* **10**, 122–132 (2013).
- Szydlowski, M., Jabłońska, E. & Juszczynski, P. FOXO1 transcription factor: a critical effector of the PI3K-AKT axis in B-cell development. *Int. Rev. Immunol.* **33**, 146–157 (2014).
- Brunet, A. et al. Akt promotes cell survival by phosphorylating and inhibiting a Forkhead transcription factor. *Cell* **96**, 857–868 (1999).
- Nakae, J. et al. The forkhead transcription factor Foxo1 regulates adipocyte differentiation. *Developmental cell* **4**, 119–129 (2003).
- Chung, S. et al. FoxO1 regulates allergic asthmatic inflammation through regulating polarization of the macrophage inflammatory phenotype. *Oncotarget* **7**, 17532 (2016).
- Chang, S. E. & Zheng, B. Q. The Role of Foxo1 In The Development and Function Of B Cells. *FASEB J.* **22**, 404–404 (2008).
- Coomes, S. et al. CD4+ Th2 cells are directly regulated by IL-10 during allergic airway inflammation. *Mucosal Immunol.* **10**, 150–161 (2017).
- Ray, A. et al. A novel IL-10-independent regulatory role for B cells in suppressing autoimmunity by maintenance of regulatory T cells via GITR ligand. *J. Immunol.* **188**, 3188–3198 (2012).
- Hsu, L.-H. et al. A B-1a cell subset induces Foxp3+ T cells with regulatory activity through an IL-10-independent pathway. *Cell. Mol. Immunol.* **12**, 354–365 (2015).
- Stanic, B. et al. IL-10-overexpressing B cells regulate innate and adaptive immune responses. *J. Allergy Clin. Immunol.* **135**, 771–780. e8 (2015).
- Matsumoto, M. et al. Interleukin-10-producing plasmablasts exert regulatory function in autoimmune inflammation. *Immunity* **41**, 1040–1051 (2014).
- Liu, C. et al. CD23 can negatively regulate B-cell receptor signaling. *Sci. Rep.* **6**, 25629 (2016).
- Liu, B. S. et al. TLR-mediated STAT3 and ERK activation controls IL-10 secretion by human B cells. *Eur. J. Immunol.* **44**, 2121–2129 (2014).
- Das, S. & Bar-Sagi, D. BTK signaling drives CD1d(hi)CD5(+) regulatory B-cell differentiation to promote pancreatic carcinogenesis. *Oncogene* **38**, 3316–3324 (2019).
- Rosser, E. C. & Mauri, C. Regulatory B cells: origin, phenotype, and function. *Immunity* **42**, 607–612 (2015).

ACKNOWLEDGEMENTS

This work was supported by National Natural Science Foundation of China (82120108013, 81801607, 81901652), the National Key R&D Program of China (2017YFA0205600), the Program for Guangdong Introducing Innovative and Entrepreneurial Teams (2017ZT07S054), and the Guangdong Basic and Applied Basic Research Foundation (2020A1515010897).

AUTHOR CONTRIBUTIONS

L.L. and Z.X.L. designed the experiments. S.R.W., R.D.H., M.M., X.Y., and L.L. performed the experiments and analyzed the data. M.M. analyzed the single cell RNA-sequencing data. S.R.W., M.M., L.L., Z.B.Z., C.S., M.E.G. and Z.X.L. wrote and edited the manuscript. H.Y.C. and Y.H. provided human samples, participated in experiment design and edited the manuscript. D.M.X. participated in experiment design and manuscript editing.

COMPETING INTERESTS

The authors declare no competing interests.

ADDITIONAL INFORMATION

Supplementary information The online version contains supplementary material available at <https://doi.org/10.1038/s41385-022-00504-z>.

Correspondence and requests for materials should be addressed to Liang Li or Zhe-Xiong Lian.

Reprints and permission information is available at <http://www.nature.com/reprints>

Publisher's note Springer Nature remains neutral with regard to jurisdictional claims in published maps and institutional affiliations.